

Are the surface Fermi arcs in Dirac semimetals topologically protected?

Mehdi Kargarian*, Mohit Randeria*, and Yuan-Ming Lu*

*Department of Physics, The Ohio State University, Columbus, OH 43210

Submitted to Proceedings of the National Academy of Sciences of the United States of America

Motivated by recent experiments probing anomalous surface states of Dirac semimetals (DSMs) Na_3Bi and Cd_3As_2 , we raise the question posed in the title. We find that, in marked contrast to Weyl semimetals, the gapless surface states of DSMs are not topologically protected in general, except on time-reversal-invariant planes of surface Brillouin zone. We first demonstrate this in a minimal 4-band model with a pair of Dirac nodes at $k = (0, 0, \pm Q)$, where gapless states on the side surfaces are protected only near $k_z = 0$. We then validate our conclusions about the absence of a topological invariant protecting double Fermi arcs in DSMs using a K-theory analysis for space groups of Na_3Bi and Cd_3As_2 . Generically, the arcs deform into a Fermi pocket, similar to the surface states of a topological insulator (TI), and this can merge into the projection of bulk Dirac Fermi surfaces as the chemical potential is varied. We make sharp predictions for the doping-dependence of the surface states of a DSM that can be tested by ARPES and quantum oscillation experiments.

Dirac semimetals | Weyl semimetals | Topological insulators | Fermi arcs

Following the theoretical prediction and experimental discovery of topological insulators [1, 2] in the past decade, there has been an explosion of interest in understanding the role of topology in various quantum states of matter. An important set of questions concerns the topological properties of *gapless* Fermi systems [3, 4, 5, 6, 7, 8]. Of particular interest are three-dimensional (3D) semimetals where the bulk electronic dispersion exhibits point nodes at the Fermi level and the low energy physics is effectively described by Weyl or Dirac Hamiltonian [9].

A striking feature of 3D Weyl semimetals (WSM), which necessarily break either time-reversal or inversion symmetry, is the existence [5] of topologically protected surface “Fermi arcs”. Here the Fermi contour in the surface Brillouin zone breaks up into disconnected pieces, which connect the projection of two Weyl nodes with opposite chirality. The Fermi arcs have been recently observed in angle-resolved photoemission spectroscopy (ARPES) studies of non-centrosymmetric TaAs [10, 11, 12, 13, 14, 15].

Here we focus on another outstanding example, the Dirac semimetal (DSM), which is the 3D analogue of graphene. In the presence of both time-reversal and inversion symmetries, the electronic excitations near each node are described by a four-component Dirac fermion, and a dispersion that is linear in all directions in \mathbf{k} -space [16, 17, 18]. ARPES has clearly observed linearly-dispersing bands near Dirac nodes in two DSM materials Na_3Bi [19, 20] and Cd_3As_2 [21, 22, 23]. The signatures of Fermi arcs by ARPES in Na_3Bi [24] and by their peculiar quantum oscillations [25] in Cd_3As_2 [26] have recently been reported. Although DSM can in principle appear in a system with spin rotational symmetry [27], here we focus on DSMs in spin-orbit-coupled systems which are more closely related to material realizations.

We can understand the Dirac fermions as two degenerate Weyl fermions with opposite chirality, where crystal symmetries forbid the two Weyl nodes from hybridizing and opening up a gap at each Dirac point [16, 28]. Given this picture of the bulk, it is natural to expect the surface states in a DSM [17, 18]

as two copies of the chiral Fermi arc on WSM surface: i.e. the “double Fermi arcs” shown schematically in Fig. 1(a).

In this paper, we address the important question of whether the double Fermi arcs on the surface of Dirac semimetals topologically protected? If yes, what is the associated topological invariant? The Fermi arcs in WSMs are robustly protected for the following reason: each plane that lies between a pair of Weyl nodes in momentum space, perpendicular to the separation between them, has an integer Chern number [5, 29, 30] associated with quantum Hall effect. The chiral edge modes of these momentum-space Chern insulators give rise to robust surface Fermi arcs, which end at the projection of bulk Weyl nodes. Unlike the WSM, the bulk-boundary correspondence in topological phase [8] provides no obvious answer for DSMs, since the stability of bulk Dirac nodes require crystal rotation symmetries [17, 18] which are explicitly broken on open side surfaces. It was claimed [25] though, that the surface Fermi arcs in DSMs are perturbatively stable against a weak symmetry-breaking surface potential, and a strong surface potential can destroy them.

Here we provide a surprising answer to the question posed in the title. We show that the double Fermi arcs on Dirac semimetal surface are *not* topologically protected, and can be continuously deformed into a closed Fermi contour without any symmetry breaking or bulk phase transition; see Fig. 1. The resulting Fermi contours do have topological character, even though they are not as exotic as the Fermi arcs in WSMs. We show that the surface states of a DSM with an odd (even) number of Dirac node pairs are analogous to the surface states of a 3D strong TI (weak TI or trivial insulator).

Significance

In recent years there has been a surge of interest in quantum materials with topologically protected properties that are robust against the effects of disorder and other perturbations. An interesting example is the newly discovered three dimensional analog of graphene, called Dirac semimetals. These were expected to have highly unusual conducting states on their surfaces. We show here that the surface states of Dirac semimetals do not exhibit the expected topological robustness and, quite generally, get deformed into states that are of a rather different character. Our theoretical results not only have conceptual importance in the field of topological quantum materials but also make clear predictions that can be tested in several experiments.

Reserved for Publication Footnotes

To make our results physically transparent, we first focus on the 4-band minimal model for DSMs [17, 18, 31] and present simple arguments for lack of topological protection for surface Fermi arcs. We then show numerical results for ARPES spectral functions for the 4-band model which demonstrates how a bulk perturbation that respects all symmetries can destroy the Fermi arcs. Next, we go beyond the simple low-energy model and directly address the two DSM materials of experimental interest. We use K-theory [4, 32, 33, 34, 35] to classify the topological stability of surface states in the presence of time reversal, charge conservation and space group symmetries in Dirac semimetals Cd₃As₂ and Na₃Bi. This classification indicates that topological protection for gapless surface states on side surfaces (that do not intersect the \hat{z} -axis) of Dirac semimetals exists only in the high-symmetry plane $k_z = 0$. We conclude by examining the experimental implications of our results. We discuss how to understand the existing ARPES and quantum oscillation measurements in light of our results on the lack of topological protection for Fermi arcs, and we make sharp predictions for testing our conclusions.

Minimal model

We begin with a simple 4-band model for a Dirac semimetal with 4-fold rotational symmetry along the \hat{z} -axis defined by the Hamiltonian:

$$H(\mathbf{k}) = \varepsilon_{\mathbf{k}}^0 + \left[t(\cos k_x + \cos k_y - 2) + t_z(\cos k_z - \cos Q) \right] \tau_z + \lambda \sin k_x \sigma_x \tau_x + \lambda \sin k_y \sigma_y \tau_x. \quad [1]$$

The Pauli matrices $\vec{\sigma}$ act on spin and $\vec{\tau}$ in orbital space, t and t_z are hopping amplitudes and λ is spin-orbit coupling (SOC). Ignoring $\varepsilon_{\mathbf{k}}^0$ for the moment, there is a gap everywhere in the Brillouin zone (BZ) except at two points $\mathbf{k} = (0, 0, \pm Q)$ where the low energy spectrum is described by linearly-dispersing Dirac fermions.

We can always add to eq. (1) an $\varepsilon_{\mathbf{k}}^0$ that preserves all the symmetries and vanishes at the Dirac nodes, e.g., $\varepsilon_{\mathbf{k}}^0 = t_1(\cos k_z - \cos Q) + t_2(\cos k_x + \cos k_y - 2)$ or $\varepsilon_{\mathbf{k}}^0 = t_1(\cos k_z - \cos Q)(\cos k_x + \cos k_y)$. While this term does not qualitatively change the Dirac spectrum in the bulk, it gives rise to a curvature of the Fermi arc in the surface BZ, as discussed below.

The symmetries of $H(\mathbf{k})$ and their representations in terms of spin and orbital operators are as follows. Time-reversal is implemented by the antiunitary operator $\Theta = i\sigma_y \cdot \mathcal{K}$, where \mathcal{K} is complex conjugation and $\Theta^2 = -1$. Inversion I corresponds to $U_I = \tau_z$, with the two orbitals having even and odd parity. Two-fold rotation $C_{2,x(y)}$ about the \hat{x} (or \hat{y}) axis is implemented by $U_{C_{2,x(y)}} = i\sigma_{x(y)}$, and n -fold rotation $C_{n,z}$ by $U_{C_{n,z}} = \exp(i\pi\sigma_z(1 - 2\tau_z)/n)$, where $n = 4$ here. $H(\mathbf{k})$ also has mirror reflection symmetries with respect to the $j = x, y, z$ -planes, with $k_j \rightarrow -k_j$, which is implemented by $U_{R_j} = U_{C_{2,j}}U_I = i\sigma_j\tau_z$.

Instability of surface Fermi arcs

Surfaces with a normal not parallel to \hat{z} -axis are expected to support gapless states with Fermi arcs, shown schematically in Fig. 1(a) for side surfaces. We address the lack of topological protection for the Fermi arcs of $H(\mathbf{k})$ from three different points of view. (i) First, we examine the stability of 1D (one-dimensional) edge states that exist on 2D slices of BZ at a fixed, generic value of k_z . Here we define a generic k_z to be $k_z \notin \{\pm Q, 0, \pi\}$, so that a fixed- k_z plane will neither contain Dirac nodes, nor will it have the additional symmetry arising from time-reversal invariance. (ii) Next, we prove the exist-

tence of an extra mass term in the gapped Dirac Hamiltonian that describes the plane with a generic k_z . (iii) Finally we show how adding fully symmetric, bulk perturbations to the 3D Hamiltonian $H(\mathbf{k})$ can destroy the Fermi arcs, without destroying the bulk Dirac nodes. The projection of these bulk nodes onto the surface does remain gapless, as do the 2D slices located at $k_z = 0$ as they have extra (time-reversal) symmetry.

Without loss of generality we consider a (100) surface. This surface preserves only the following symmetries: time reversal Θ , mirror reflections R_y, R_z and their combinations. Therefore a fixed- k_z plane in a system with with a (100) surface only respects two symmetry operations: mirror reflection $U_{R_y} = i\sigma_y\tau_z$ w.r.t. \hat{y} -plane, and the combination $\Theta_{R_z} = \Theta U_{R_z} = i\sigma_x\tau_z \cdot \mathcal{K}$ of time reversal and mirror w.r.t. \hat{z} -plane. Note that $\Theta_{R_z}^2 = 1$. Under these symmetries the Hamiltonian at fixed k_z , denoted by $\tilde{H}(k_x, k_y)$, transforms as $\Theta_{R_z}^{-1}\tilde{H}(k_x, k_y)\Theta_{R_z} = \tilde{H}(-k_x, -k_y)$ and $U_{R_y}^{-1}\tilde{H}(k_x, k_y)U_{R_y} = \tilde{H}(k_x, -k_y)$.

(i) First consider the surface BZ (k_y, k_z) for a (100) surface. If we look at a 1D slice at fixed- k_z where we might have expected gapless edge states described by $H_{\text{edge}} = \hbar v_F \sum_{k_y} \psi_{k_y}^\dagger (k_y \mu_z - k_F) \psi_{k_y}$. Here $\psi_{k_y}^T = (\psi_{R,k_y}, \psi_{L,k_y})$ is a two-component spinor of right (R) and left (L) movers and $\vec{\mu}$ are Pauli matrices in (R, L) -space. Note that the dispersion v_F and the location of the Fermi arc k_F are both, in general, k_z -dependent.

The two symmetry operations on the edge states are represented by $\Theta_{R_z} = i\mu_x \cdot \mathcal{K}$ and $U_{R_y} = i\mu_y$. We now add perturbation $\hat{M} = m \sum_{k_y} \psi_{k_y}^\dagger \mu_y \psi_{k_y}$, which preserves both these surface symmetries: $[\Theta_{R_z}, \mu_y] = [U_{R_y}, \mu_y] = 0$. Clearly \hat{M} is a mass term for H_{edge} that destroys the gapless edge states.

(ii) Next, we gain insight into the instability of surface states on a fixed- k_z plane within classification scheme [32, 33, 34] of topological insulators. For a fixed, generic k_z , our system is a gapped 2D insulator described by a Dirac Hamiltonian

$$\tilde{H}_D = k_x \gamma_x + k_y \gamma_y + m \gamma_0, \quad [2]$$

up to an additive constant term. Here $\gamma_x = \sigma_x \tau_x$, $\gamma_y = \sigma_y \tau_x$ and $\gamma_0 = \tau_z$ are Dirac matrices in the minimal model. Let us ask if we can add another mass term $m' \gamma'_0$ to \tilde{H}_D which preserves all the symmetries and anti-commutes with all the Dirac matrices $\gamma_{x,y,0}$. If we can do this, the $m > 0$ phase can be continuously deformed into the $m < 0$ phase without closing the gap at $m = 0$, and \tilde{H}_D would be topologically trivial. Such a term indeed exists: $\gamma'_0 = \sigma_z \tau_x$ commutes with Θ_{R_z} and U_{R_y} and anticommutes with $\gamma_{x,y,0}$. Therefore the surface states at generic k_z are not topologically protected.

In contrast to generic k_z , the time-reversal-invariant planes $k_z = 0$ and $k_z = \pi$ are gapped 2D insulators with the well-known \mathbb{Z}_2 topological index associated with quantum spin Hall (QSH) effect [1, 2]. In the DSM materials Cd₃As₂ and Na₃Bi, there is a nonsymmorphic glide reflection g_c containing half-translation along \hat{z} -axis, which serves as a mirror reflection for $k_z = 0, \pi$ planes satisfying $(g_c)^2 = -1(+1)$ for $k_z = 0(\pi)$. Generically such nonsymmorphic glide reflections guarantees that the \mathbb{Z}_2 index must be trivial for the $k_z = \pi$ plane [36], which will be elaborated below. Therefore in these materials, only $k_z = 0$ plane can support a nontrivial \mathbb{Z}_2 index. A simple calculation [37] shows that the $k_z = 0$ plane is indeed a nontrivial QSH insulator, and gapless surface states at $k_z = 0$ are topologically protected.

(iii) Finally we directly examine the gapless surface states of the 3D Hamiltonian (1) in a slab geometry with a surface at $x = 0$, which is translationally invariant along y and z . We numerically calculate the spectral density $A(\mathbf{k}, \omega) =$

$-(1/\pi)\text{Im}G(\mathbf{k}, \omega + i0^+)$ associated with the electron Green function $G(\mathbf{k}, \omega)$. Here we measure ω with respect to the zero chemical potential, which coincides with the bulk Dirac nodes. We show in Fig. 1 the surface [panels (b,c,d)] contributions to $A(\mathbf{k}, 0)$ as a function of in-plane momentum (k_y, k_z). Note that ARPES probes precisely this spectral density multiplied by the Fermi-Dirac function.

In Fig. 1(b), we plot the result for $H(\mathbf{k})$ of eq. (1) and clearly see the two Fermi arcs extending from one Dirac node to the other. In the absence of the $\varepsilon_{\mathbf{k}}^0$ term of the form discussed above, $H(\mathbf{k})$ has an (unnatural) “chiral symmetry” and the two Fermi arcs become “degenerate” and collapse to $k_y = 0$ for $-Q < k_z < Q$ [38]. With $\varepsilon_{\mathbf{k}}^0$ in place, we get the arcs shown in Fig. 1(b).

Now we ask if there is a perturbation that has the full symmetry, does not shift the bulk nodes and yet has a $\sigma_\alpha \otimes \tau_\beta$ structure that anticommutes with each term in $H(\mathbf{k})$ (other than the $\varepsilon_{\mathbf{k}}^0$ term, of course). Such a perturbation does exist and it must be of the form

$$\delta H_4(\mathbf{k}) = m'(\cos k_x - \cos k_y) \sin k_z \sigma_z \tau_x \quad [3]$$

This perturbation destroys the Fermi arcs near the projections of the Dirac nodes at $k_z = \pm Q$ on to the surface BZ as shown in Fig. 1. We clearly see this in panel (c) where $\delta H_4(\mathbf{k})$ with $m' = 0.4t$ deforms the Fermi arcs into a closed Fermi pocket. An increase in the strength of the perturbation to $m' = 0.8t$ shrinks the arcs to even smaller pockets as shown in Fig. 1(d). While the surface Fermi arcs are progressively destroyed, the bulk Dirac nodes (and bulk states near $E_F = 0$) are unaffected by these perturbations. We note that this perturbation of $\mathcal{O}(k^3)$ is higher order than that retained in usual $\mathbf{k} \cdot \mathbf{p}$ perturbation theory.

The minimal 4-band model [31] is equivalent, up to a unitary transformation [38], to the well-known effective $\mathbf{k} \cdot \mathbf{p}$ Hamiltonian around the Γ point for DSM materials [17, 18]. Despite its simplicity, this model with $n = 4$ -fold rotational symmetry about the \hat{z} -axis captures the band inversion near the Γ point of BZ in Cd_3As_2 . A similar model can also be adopted for the case of Na_3Bi with $n = 6$ -fold rotational symmetry [38].

K-theory

Using K-theory we next show that the surface states and associated Fermi arcs in Cd_3As_2 and Na_3Bi are not topologically protected. This mathematical framework has the great advantage of focusing only on the space group, $U(1)$ charge conservation and time reversal symmetry of a material, without the need for a low-energy effective model such as the one used in the analysis above. We thus obtain general and rigorous results that are directly applicable to real materials.

In the K-theory approach [32, 33, 34], the classification of distinct gapped symmetric phases is reduced to the following mathematical problem: what is the “classifying space” of symmetry-allowed mass matrix for a generic Dirac Hamiltonian preserving certain symmetries? Different symmetric phases correspond to disconnected pieces of the classifying space, which cannot be continuously connected to each other without closing the bulk energy gap. Mathematically the group structure formed by these different phases is given by the zeroth homotopy group $\pi_0(S)$ of classifying space S . Here we only sketch the idea behind the calculations; detailed analysis are given in Supplementary Materials [38].

Na₃Bi: The hexagonal DSM material Na_3Bi has a unit cell is defined by $\mathbf{a} = a(1, 0, 0)$, $\mathbf{b} = a(-1/2, \sqrt{3}/2, 0)$ and $\mathbf{c} = c(0, 0, 1)$. Its space group is centrosymmetric $P6_3/mmc$ (No. 194) [17], with its symmetry operations are generated

by 6-fold screw $s_6: (x, y, z) \rightarrow (x - y, x, z + 1/2)$, glide reflection $g_c: (x, y, z) \rightarrow (y, x, z + 1/2)$, inversion $I: (x, y, z) \rightarrow (-x, -y, -z)$, and Bravais lattice translations $T_{a,b,c}$.

The two Dirac nodes [17] in Na_3Bi are located at $\mathbf{Q}_\pm = \pm Q_0(2\pi/c)(0, 0, 1)$. We consider two different surfaces which can potentially contain nontrivial Fermi arcs. (i) A (010) surface spanned by the \mathbf{a} and \mathbf{c} axes, and (ii) a (110) surface spanned by $(\mathbf{a} - \mathbf{b})$ and \mathbf{c} . In each case we proceed as follows. We begin by determining the reduced set of symmetries that are preserved in the presence of the surface. By analyzing how these symmetries act on a general Bloch Hamiltonian, we determine those symmetries that preserve a 2D plane in the BZ zone at a fixed value of $k_z \neq 0, \pi/c$. All such planes, except those passing through the nodes at \mathbf{Q}_\pm are fully gapped.

The basic strategy is to exploit the classification of gapped insulators described by Dirac Hamiltonians defined on these 2D planes embedded in the 3D Brillouin zone. We use the K-theory classification [32, 33, 34] of gapped free-fermion quantum phases by examining the combined algebra for the Dirac γ -matrices and the symmetry operations and determining whether the *classifying space* for symmetry-allowed mass terms is connected or not.

Using this approach we conclude that a generic 2D plane in the BZ at fixed k_z is topologically trivial and does not need to support protected surface states. The plane $k_z = \pi/c$ is also shown to be trivial, due to the presence of the nonsymmorphic glide reflection g_c . Only the $k_z = 0$ plane is found to have a nontrivial \mathbb{Z}_2 QSH index.

Cd₃As₂: The space group of the tetragonal DSM Cd_3As_2 is centrosymmetric $I4_1/acd$ (No. 142) [39]. In addition to Bravais lattice translations, its symmetry operations are generated by 4-fold screw rotation along \hat{z} -axis: $(x, y, z) \rightarrow (y, 1/2 - x, 1/4 + z)$, glide reflection $g_c: (x, y, z) \rightarrow (x, -y, 1/2 + z)$, and inversion $I: (x, y, z) \rightarrow (-x, 1/2 - y, 1/4 - z)$, where $(s_4)^4 = (g_c)^2 = -T_z$. The Bravais lattice is expanded by $T_{\pm 1, \pm 1, \pm 1} \equiv (\pm 1, \pm 1, \pm 1)/2$ similar to BCC lattice. The two Dirac nodes in Cd_3As_2 are located along the \hat{z} -axis.

The K-theory procedure is used to determine the topological nature of various 2D planes in the BZ at fixed k_z , in a manner completely analogous to that described above, taking into account of the symmetries of Cd_3As_2 . The calculations are described in supplementary materials [38], and the conclusions are identical to the ones given above. Only the $k_z = 0$ plane has a nontrivial \mathbb{Z}_2 QSH index, all other fixed k_z planes are trivial.

Nature of Surface States

We next show that the closed Fermi pocket on a side surface is essentially the same as the surface Dirac fermion of a 3D strong topological insulator (TI). Consider a weak perturbation that breaks C_n symmetry, but preserves time reversal and inversion. We require the strength of this perturbation is smaller than the bulk gap at the time reversal invariant momenta (TRIM) of the 3D BZ. Clearly this perturbation will gap out the Dirac nodes but will not affect of parity eigenvalues of filled bands at the TRIM. Now that the bulk is fully gapped band insulator with time reversal symmetry, its \mathbb{Z}_2 topological invariant is given by the number of odd-parity Kramers pairs in filled bands at TRIM as shown by Ref. [37]. Since the $k_z = 0$ plane is a 2D QSH insulator and $k_z = \pi$ is a trivial 2D insulator, the gapped bulk must be in a 3D strong TI phase. In the process of turning on the perturbation, the surface states at $k_z = 0$ remain gapless since time reversal is always preserved. This demonstrates the equivalence between the closed Fermi pocket for DSMs and surface Dirac fermions of strong TIs.

An important conclusion from our analysis is that if the bulk band touching occurs at an odd number of pairs of Dirac nodes not located at TRIM (such as in Cd_3As_2 and Na_3Bi), then the surface states cannot be fully removed due to time reversal symmetry. Let N_p Dirac points be located in the top half of the bulk BZ ($0 < k_z < \pi$) and their N_p time-reversal counterparts in the bottom half BZ ($-\pi < k_z < 0$). Based on our arguments, this will lead to N_p closed Fermi pockets on a generic surface, which are either centered around $k_z = 0$ or $k_z = \pi$. If there are an odd number of Fermi pockets centered around $k_z = 0$, the gapped $k_z = 0$ plane in 1st BZ must correspond to a 2D QSH insulator with an odd number of helical edge states. Therefore, if N_p is odd, $k_z = 0$ and $k_z = \pi$ must have opposite Z_2 topological indices, with one plane being a trivial 2D insulator and the other a QSH insulator. Hence the surface states of an odd- N_p DSM cannot be fully gapped out, in complete analogy with a 3D strong TI. On the other hand, if N_p is even, both the $k_z = 0$ and $k_z = \pi$ planes share the same Z_2 index i.e. they are both trivial 2D insulators or both QSH insulators. In the former case there are generally no surface states, while gapless surface states in the latter case can be gapped out by translation symmetry breaking perturbations in analogy to a 3D weak TI. As a result, an “odd DSM” with an odd number of pairs of Dirac points must support time-reversal-protected gapless surface states, in contrast to an “even DSM”, whose surface states can either be fully gapped or need protection from crystal translation symmetry.

Experimental Implications

We have shown above that, in general, the surface states of Dirac semimetals Cd_3As_2 and Na_3Bi have a closed Fermi surface (FIG. 1 (c)), in contrast to the double Fermi arcs that one might naively expect (FIG. 1 (b)). We now address the important question of how one can experimentally distinguish between these two types of surface states.

Assume, first, for simplicity that the chemical potential is at the Dirac point; (we discuss below the case when it is not). The qualitative differences between the two outcomes are then as follows. The double Fermi arc has a singular change in slope when two arcs meet at the projection of a Dirac node on to the surface BZ. In contrast, a Fermi contour has a smooth curvature everywhere in the surface BZ and it does not pass through the two points that are the projections of the bulk Dirac nodes. In addition, the wave-function associated with the surface states merges with the bulk at the tip of the arc, namely the Dirac node; in contrast the states associated with a regular Fermi contour are exponentially localized at the surface. All of these features could, in principle, be used to distinguish between the two scenarios using sufficiently high-resolution ARPES data with photon energy dependence used to separate bulk and surface contributions.

We next consider the very interesting quantum oscillation experiments on Cd_3As_2 thin films [26]. The observed Shubnikov-de Haas oscillations seem consistent with “Weyl orbits”, which consist of the combination of bulk Landau levels (LLs) and surface Fermi arcs [25]. How can we understand these experimental results, if the surface states have a closed Fermi pocket instead of double Fermi arcs?

First of all, both transport [40, 41, 26] and ARPES [42, 22] experiments confirmed that Cd_3As_2 is slightly n-doped, in the sense that Fermi energy E_F lies above the Dirac points with $k_F \simeq 0.04\text{\AA}^{-1}$. Therefore the surface projection of the bulk electronic states, near each Dirac point, is in fact a small “blob” denoted by a red oval in FIG. 1 (d)-(f). In this case, the surface states at the Fermi energy may (FIG. 1(f)) or may not (FIG. 1(e)) be connected with the bulk Fermi blobs, de-

pending on E_F . When the surface pocket merges into the bulk blobs, the magnetic orbits responsible for quantum oscillations must be the Weyl orbits proposed in Ref. [25] which consists of both bulk LLs and surface Fermi arcs. Shubnikov-de Haas oscillations in Ref. [26] suggest that this is the situation in Cd_3As_2 . The available ARPES results in Na_3Bi [24] are also consistent with surface states merging into bulk projection as k_z increases.

However if we start to introduce p-type dopants to the system and lower the Fermi level, ultimately the surface pocket must get disconnected from the bulk blobs, as shown in FIG. 1 (d)-(e), when the Fermi level is close enough to the Dirac points. In this case the surface Fermi pocket will provide a closed 2D magnetic orbit for cyclotron motion. This pocket is analogous to the 2D Dirac fermion on the surface of topological insulators (TIs) and will lead to quantum oscillations similar to those observed in TIs [43, 44, 45], with the electron acquiring a Berry phase of π as it goes around the Fermi contour. As with any 2D Fermi surface, the quantum oscillation frequency F_s has a $1/\cos\theta$ dependence on the angle θ between magnetic field and surface normal direction. There is an important difference between the quantum oscillations in the two scenarios where the bulk and surface states are mixed and separated is that in the latter case, F_s has no dependence on the thickness of the sample, in sharp contrast to the Weyl orbits [25, 26] in the former.

Therefore quantum oscillation experiments at different doping levels provide a sharp distinction between double Fermi arcs and TI-like closed surface Fermi pockets, serving as an experimental test of our conclusion. There will be two frequencies in quantum oscillations on DSM thin films [25, 26]: F_b associated with bulk Fermi surfaces (due to deviation of E_F from Dirac point) and F_s related to the surface states. As we move E_F towards bulk Dirac points by doping the system, F_b will always decrease monotonically. As demonstrated in Ref. [26], a triangle-shaped sample does not exhibit quantum oscillations with frequency F_s , while a rectangular sample does, because the Weyl orbits depend on the thickness of the system along the field direction. Thus in a triangle-shaped sample, double Fermi arcs cannot lead to quantum oscillation at F_s independent of the Fermi level. On the other hand, as the surface pocket is disconnected from the bulk blobs by tuning E_F close to the Dirac point (see FIG. 1(e)), the frequency F_s , with a 2D angular-dependence, will show up even in a triangular sample. In particular, when the magnetic length $l_B = \sqrt{\hbar/eB}$ satisfies $k_d \gg l_B^{-1}$ where k_d is the shortest distance between the surface pocket and the bulk blob in surface BZ, the closed surface pocket cannot tunnel into bulk LLs to form a closed Weyl orbit. When the Fermi level lies exactly at the Dirac point, $k_d \sim 0.04\text{\AA}^{-1}$ gives an estimate of $B < 10^2 T$ which is within the experimental reach. Of course, very high-resolution ARPES studies can also directly reveal the separation of surface Fermi pocket from the bulk blobs as the photon energy is varied.

Concluding remarks

Let us conclude by summarizing our main results. Each bulk Dirac node looks like two copies of a Weyl node, which naively suggests that the surface electronic structure of a DSM should look like two copies of that of the Weyl semimetal (WSM), namely a double Fermi arc. We show here – using a simple 4-band model and rigorous K-theory calculations – that the double Fermi arcs are not topologically protected, unlike the Fermi arc in a WSM. We find that an arbitrarily small bulk perturbation, which preserves the Dirac nodes and all the symmetries, can lead to a deformation of the double Fermi arc into

a more conventional Fermi contour. Nevertheless, we show that the surface states in a DSM cannot be completely destroyed, because there must be topologically protected states on the $k_z = 0$ plane, similar to a 3D TI.

Finally, we explore in detail the experimental implications of our results. We show how we can reconcile our results on the lack of topological protection with existing experiments on Na₃Bi [24] and Cd₃As₂ [26]. While these have been interpreted as being consistent with Fermi arcs, we argue that they are actually a consequence of the mixing of bulk and surface

states. We also propose hole-doping the system to disconnect the surface Fermi pocket and bulk states, and suggest testable signatures for both ARPES and quantum oscillation experiments.

SI-only references:[46, 47, 48]

ACKNOWLEDGMENTS. MK and MR acknowledge the support of the CEM, an NSF MRSEC, under grant DMR-1420451. YML thanks the Aspen Center for Physics for hospitality, where part of the manuscript was written. YML acknowledges support from startup funds at Ohio State University, and in part from NSF grant PHY-1066293.

1. Hasan MZ, Kane CL (2010) Colloquium: Topological insulators. *Rev. Mod. Phys.* 82:3045–3067.
2. Qi XL, Zhang SC (2011) Topological insulators and superconductors. *Rev. Mod. Phys.* 83:1057–1110.
3. Volovik GE (2003) *The Universe in a Helium Droplet* (Clarendon Press, Oxford, England).
4. Horava P (2005) Stability of fermi surfaces and k theory. *Phys. Rev. Lett.* 95:016405–.
5. Wan X, Turner AM, Vishwanath A, Savrasov SY (2011) Topological semimetal and fermi-arc surface states in the electronic structure of pyrochlore iridates. *Phys. Rev. B* 83:205101.
6. Burkov AA, Hook MD, Balents L (2011) Topological nodal semimetals. *Phys. Rev. B* 84:235126.
7. Zhao YX, Wang ZD (2013) Topological classification and stability of fermi surfaces. *Phys. Rev. Lett.* 110:240404–.
8. Matsuura S, Chang PY, Schnyder AP, Ryu S (2013) Protected boundary states in gapless topological phases. *New Journal of Physics* 15:065001–.
9. Vafeek O, Vishwanath A (2014) Dirac fermions in solids: From high- T_c cuprates and graphene to topological insulators and weyl semimetals. *Annual Review of Condensed Matter Physics* 5:83–112.
10. Xu SY, et al. (2015) Discovery of a weyl fermion semimetal and topological fermi arcs. *Science* 349:613–617.
11. Weng H, Fang C, Fang Z, Bernevig BA, Dai X (2015) Weyl semimetal phase in noncentrosymmetric transition-metal monophosphides. *Phys. Rev. X* 5:011029.
12. Huang SM, et al. (2015) A weyl fermion semimetal with surface fermi arcs in the transition metal monopnictide taas class. *Nat Commun* 6:7373.
13. Lv BQ, et al. (2015) Experimental discovery of weyl semimetal taas. *Phys. Rev. X* 5:031013.
14. Lv BQ, et al. (2015) Observation of weyl nodes in taas. *Nat Phys* 11:724–727.
15. Xu SY, et al. (2015) Discovery of a Weyl fermion state with Fermi arcs in niobium arsenide *Nat Phys* 11:748–754.
16. Young SM, et al. (2012) Dirac semimetal in three dimensions. *Phys. Rev. Lett.* 108:140405.
17. Wang Z, et al. (2012) Dirac semimetal and topological phase transitions in $A_3\text{Bi}$ ($A = \text{Na}, \text{K}, \text{Rb}$). *Phys. Rev. B* 85:195320.
18. Wang Z, Weng H, Wu Q, Dai X, Fang Z (2013) Three-dimensional dirac semimetal and quantum transport in Cd_3As_2 . *Phys. Rev. B* 88:125427.
19. Liu ZK, et al. (2014) Discovery of a three-dimensional topological dirac semimetal, Na_3Bi . *Science* 343:864–867.
20. Xiong J, et al. (2015) Anomalous conductivity tensor in the dirac semimetal Na_3Bi . [arXiv:1502.06266](https://arxiv.org/abs/1502.06266).
21. Yi H, et al. (2014) Evidence of topological surface state in three-dimensional dirac semimetal Cd_3As_2 . *Sci. Rep.* 4:6106.
22. Neupane M, et al. (2014) Observation of a three-dimensional topological dirac semimetal phase in high-mobility Cd_3As_2 . *Nat Commun* 5:3786
23. Jeon S, et al. (2014) Landau quantization and quasiparticle interference in the three-dimensional dirac semimetal Cd_3As_2 . *Nat Mater* 13:851–856.
24. Xu SY, et al. (2015) Observation of fermi arc surface states in a topological metal. *Science* 347:294–298.
25. Potter AC, Kimchi I, Vishwanath A (2014) Quantum oscillations from surface fermi arcs in weyl and dirac semimetals. *Nat Commun* 5:5161.
26. Moll PJ, et al. (2015) Chirality transfer dynamics in quantum orbits in the dirac semi-metal Cd_3As_2 . [arXiv:1505.02817](https://arxiv.org/abs/1505.02817).
27. Morimoto T, Furusaki A (2014) Weyl and dirac semimetals with F_2 topological charge. *Phys. Rev. B* 89:235127.
28. Yang BJ, Nagaosa N (2014) Classification of stable three-dimensional dirac semimetals with nontrivial topology. *Nat Comm* 5:4898.
29. Yang KY, Lu YM, Ran Y (2011) Quantum hall effects in a weyl semimetal: Possible application in pyrochlore iridates. *Phys. Rev. B* 84:075129–.
30. Yang BJ, Nagaosa N (2014) Emergent topological phenomena in thin films of pyrochlore iridates. *Phys. Rev. Lett.* 112:246402.
31. Chiu CK, Schnyder AP (2015) Classification of crystalline topological semimetals with an application to Na_3Bi . *Journal of Physics: Conference Series* 603:012002.
32. Kitaev A (2009) Periodic table for topological insulators and superconductors. *AIP Conference Proceedings* 1134:22–30.
33. Wen XG (2012) Symmetry-protected topological phases in noninteracting fermion systems. *Phys. Rev. B* 85:085103–.
34. Morimoto T, Furusaki A (2013) Topological classification with additional symmetries from clifford algebras. *Phys. Rev. B* 88:125129–.
35. Shiozaki K, Sato M (2014) Topology of crystalline insulators and superconductors. *Phys. Rev. B* 90:165114.
36. Varjas D, Juan Fd, Lu YM (2015) Space group constraints on weak indices in topological insulators. [arXiv:1603.04450](https://arxiv.org/abs/1603.04450).
37. Fu L, Kane CL (2007) Topological insulators with inversion symmetry. *Phys. Rev. B* 76:045302.
38. (2016) See Supplemental Materials for details.
39. Ali MN, et al. (2014) The crystal and electronic structures of Cd_3As_2 , the three-dimensional electronic analogue of graphene. *Inorganic Chemistry* 53:4062–4067.
40. Rosenman I (1969) Effet shubnikov de haas dans Cd_3As_2 : Forme de la surface de fermi et modele non parabolique de la bande de conduction. *Journal of Physics and Chemistry of Solids* 30:1385 – 1402.
41. He LP, et al. (2014) Quantum transport evidence for the three-dimensional dirac semimetal phase in Cd_3As_2 . *Phys. Rev. Lett.* 113:246402.
42. Borisenko S, et al. (2014) Experimental realization of a three-dimensional dirac semimetal. *Phys. Rev. Lett.* 113:027603.
43. Ren Z, Taskin AA, Sasaki S, Segawa K, Ando Y (2010) Large bulk resistivity and surface quantum oscillations in the topological insulator $\text{Bi}_2\text{Te}_2\text{Se}$. *Phys. Rev. B* 82:241306–.
44. Qu DX, Hor YS, Xiong J, Cava RJ, Ong NP (2010) Quantum oscillations and hall anomaly of surface states in the topological insulator Bi_2Te_3 . *Science* 329:821–824.
45. Analytis JG, et al. (2010) Two-dimensional surface state in the quantum limit of a topological insulator. *Nat Phys* 6:960–964.
46. Voon LCLY, Willatzen M (2009) *The $k \cdot p$ Method: Electronic Properties of Semiconductors* (Springer).
47. Yu P, Cardona M (2010) *Fundamentals of Semiconductors: Physics and Materials Properties*, Graduate Texts in Physics (Springer), 4th edition.
48. Sancho MPL, Sancho JML, Sancho JML, Rubio J (1985) Highly convergent schemes for the calculation of bulk and surface green functions. *Journal of Physics F: Metal Physics* 15:851.

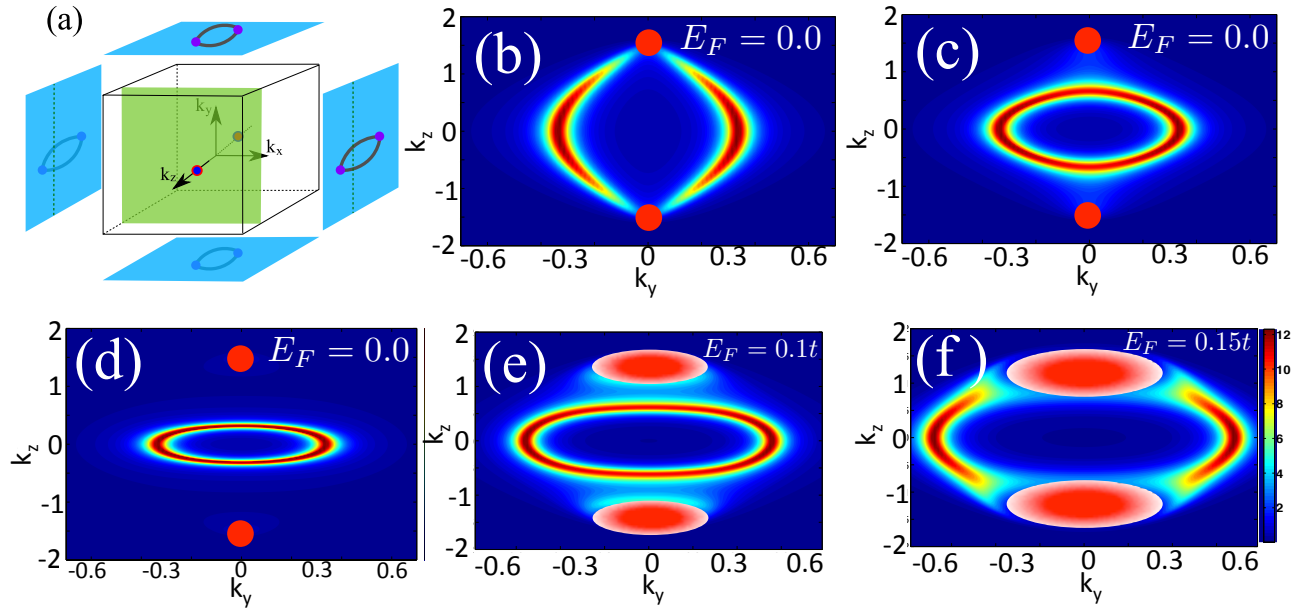


Fig. 1. (Color online) (a) Schematic \mathbf{k} -space picture of a Dirac semimetal showing Dirac nodes along k_z axis in bulk Brillouin zone (BZ) and possible double Fermi arcs on the surface BZ's, shown as blue squares. Note that surfaces perpendicular to z axis have no arcs. A 2D slice of the bulk BZ perpendicular to k_z axis is shown as a green square, which projects to a green dashed line on a side surface. (b) Surface spectral density of model in (1), which clearly shows the existence of double Fermi arcs on (100) surface. (c,d) Continuous deformation of double Fermi arcs on the (100) surface by adding the perturbation $\delta H_4(\mathbf{k})$ to (1). (c) shows the effect at $m' = -0.4t$, while (d) corresponds to $m' = -0.8t$, showing that the Fermi arcs are progressively destroyed by increasing strength of perturbation. The red solid circles in (b-d) correspond to the projection of bulk nodes and we set $E_F = 0$ to line up the Fermi level with bulk Dirac nodes. (e,f) correspond to electron doped systems with $m' = -0.8t$ (case in d) by raising the Fermi energy to $E_F = 0.1t$ and $E_F = 0.15t$, respectively. The large red blobs in (e,f) mark the projection of bulk states onto the surface BZ. The Fermi contour of the surface states is disconnect from the blobs in panel (e), while it merges into the bulk states in panel (f).